Large Eddy Simulation of Wave-driven Hydrodynamics through Emergent Aquatic Vegetation

V. Etminan[1,2], R.J. Lowe[2,3,4] and M. Ghisalberti[1,5]

[1]School of Civil, Environmental and Mining Engineering,
The University of Western Australia, Perth, Western Australia, Australia

[2]School of Earth and Environment,
The University of Western Australia, Perth, Western Australia, Australia

[3]UWA Oceans Institute, University of Western Australia, Perth,
Western Australia, Australia

[4]ARC Centre of Excellence for Coral Reef Studies,
University of Western Australia, Perth, Western Australia, Australia

[5]Department of Infrastructure Engineering, The University of Melbourne,
Parkville, Victoria, Australia

Abstract

Vegetation in coastal wetlands provides natural protection against storm surges and extreme waves. The capacity of this aquatic vegetation to attenuate waves reaching a coastline depends on the extent to which wave energy is dissipated by small-scale hydrodynamic interactions within a canopy, which is often parameterised using a drag coefficient C_d. Existing models for predicting C_d are usually dependent solely on flow characteristics and neglect the hydrodynamic impact of adjacent stems. In this study, the flow structure inside a canopy under wave-driven oscillatory flow conditions is examined numerically to investigate the mechanisms that govern drag forces and wave dissipation by emergent vegetation. Large Eddy Simulations of oscillatory flow through an emergent canopy, modelled as an array of rigid cylinders, show that the streamwise force exerted on a cylinder inside an array is different to that of a single cylinder, to an extent that depends on values of the Keulegan-Carpenter and Reynolds numbers. Moreover, vorticity and velocity fields reveal that the structure of the flow around a single cylinder is altered by the presence of neighbouring cylinders at array densities typical of coastal vegetation stands. The results of this study are beneficial for developing improved models for vegetation-induced wave attenuation.

Introduction

Coastal vegetation provides a wide range of ecosystem services, such as the reduction of coastal erosion, provision of habitat and enhancement of local water quality. The capacity for coastal vegetation to act as a natural form of coastal protection by attenuating incident waves has been the subject of numerous recent studies [2, 6, 9, 24]. Despite many efforts to quantify the vegetation-induced wave attenuation, there is still a lack of understanding of the small-scale mechanisms responsible for energy dissipation within canopies and how to best parameterise these processes; for example, in practical coastal engineering models. An understanding of these mechanisms is key to the development of reliable models for vegetation-induced wave attenuation.

Wave attenuation by vegetation is a large-scale process (often occurring over hundreds of meters) that relies on small-scale interactions between vegetation stems and fluid particles [24]. Canopy wave attenuation is quantified in large-scale coastal models through incorporation of simplified vegetation models. An effective vegetation model must correctly incorporate vegetation characteristics as well as wave parameters. Early models simulated the effect of vegetation through an increased bed friction coefficient [3, 18]; however, more recent efforts attempt to predict wave attenuation using the conservation of wave energy equation and account for vegetation effects through an energy dissipation term [4, 14] or by employing conservation of momentum [10, 11]. Both of these approaches represent vegetative resistance using a drag coefficient, C_d.

The drag coefficient depends on both flow and vegetation parameters and different models for C_d, based largely on highly empirical relationships that generally do not adequately capture many key aspects of the physical processes. The drag coefficient of a cylinder in oscillatory flow is known to depend on two key dimensionless parameters; namely, the Reynolds number ($Re = U_m d/\nu$ where U_m is the amplitude of horizontal orbital velocity, d is the cylinder diameter and ν is kinematic viscosity) [7, 17] and Keulegan–Carpenter number ($KC = U_m T/d$ where T is the wave period) [8, 14]. However, none of the proposed models consider how vegetation characteristics physically modify C_d. Despite some efforts to incorporate vegetation characteristics such as flexibility [6, 24] into drag coefficient models, improving the reliability of estimates of C_d for real vegetation canopies is an area of ongoing research.

A successful drag coefficient model relies on an insight into the flow structures inside the canopy [12]. Unlike unidirectional flow through vegetated canopies, which has been extensively investigated, studies on the oscillatory flow structure are rare [13]. In this study, Large Eddy Simulations of oscillatory flow through an emergent canopy, modelled as an array of rigid cylinders, with a solid fraction of $\lambda = 0.12$ at (Re, KC) = (100, 5), (500, 10) and (1000, 50) were investigated. Drag and inertia coefficients of cylinders inside the array were quantified and contrasted against those of a single cylinder. Furthermore, the oscillatory flow structures such as pressure, vorticity and velocity fields inside the array were analysed.

Methodology

Large Eddy Simulations (LES) of flow through staggered arrays of circular cylinders were conducted using the open source computational fluid dynamics package OpenFOAM [22]. The

computational domain includes 12 cylinders; however, to mimic an infinite array of cylinders, cyclic boundary conditions were imposed in the streamwise and transverse directions (Figure 1). At the bed and around the cylinder surfaces, a no-slip condition was applied. In order to avoid the complexity of modelling the water free surface, the upper boundary of the domain was treated as a frictionless rigid lid. The cylinder spacing was chosen such that the density of the array λ was 0.12. The water depth was $10d$. The grid topology consists of O-grid blocks around the cylinders and Cartesian H-grid blocks (similar to [19]). The H-grid was uniform in the horizontal plane but the grid of the O-grid block was concentrated toward the cylinder. In the vertical direction, the mesh was concentrated near the bed to resolve the wave boundary layer.
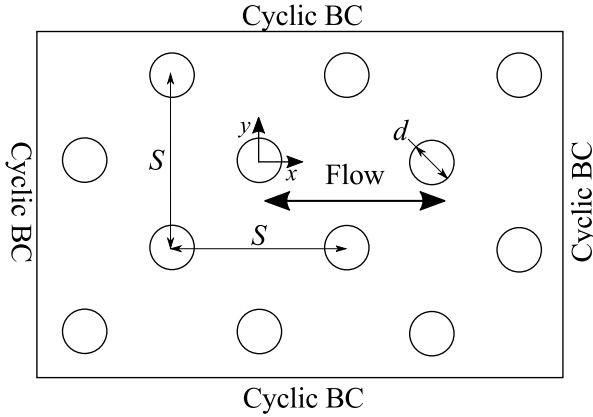
Figure 1 Schematic diagram of the computational domain and cylinder arrangement

The oscillating flow velocity in the computational domain was imposed using a momentum source as

$$u_1 = U_m \cos(2\pi t/T), \ \ u_2 = 0, \ \ u_3 = 0 \tag{1}$$

where t is time and u_1 and u_2 are the velocity components in the streamwise and transverse directions, respectively. In this study, U_m represents the amplitude of the streamwise oscillatory velocity averaged over the pore spaces between cylinders. Equation (1) indicates that the imposed velocity does not vary with elevation, which is the case for shallow water waves where $kh \ll 1$ (k is the wave number and h is water depth). The streamwise force exerted on each cylinder under the imposed oscillatory motion is conventionally expressed by the Morison equation [15]:

$$F_1 = \frac{1}{2}\rho C_d h d u_1 |u_1| + \frac{1}{4}\rho C_m h \pi d^2 \dot{u}_1 \tag{2}$$

where ρ is the fluid density and C_d and C_m are the drag and inertia coefficients, respectively. A least-squares method [23] was used in this study to determine the drag and inertia coefficients based on the time series of streamwise force exerted on each cylinder. In addition to the simulations of oscillatory flow through an array of cylinders, results of simulations of unidirectional flow around single (isolated) cylinders and arrays and also oscillatory flows around a single (isolated) cylinder are presented for comparison.

Experimental results of the force coefficients of a single cylinder in oscillatory flow are used here to validate the numerical methodology employed here. For $(KC, Re) = (100,5)$, our LES results for oscillatory flow around a single cylinder yield $C_d = 2.08$ and $C_m = 2.35$. These values are very close to the values of $C_d = 2.10$ and $C_m = 2.45$ reported in previous studies [5, 16, 21].

Results and Discussion

Drag and Inertia Coefficients

Table 1 shows the drag (C_d) and inertia coefficients (C_m) obtained in this study. Under unidirectional flow (i.e. $KC \rightarrow \infty$), cylinders in arrays have significantly higher drag coefficients than a single cylinder [20]. In oscillatory flow, the C_d values of cylinders in arrays are slightly higher than that of a single cylinder, except for $(KC, Re) = (10,500)$. In addition, it can be seen that the ratio of the inertia coefficient of a cylinder in an array to that of a single cylinder increases with Re and KC.

		Single cylinder		Cylinder in array	
Re	KC	C_d	C_m	C_d	C_m
100	5	2.08	2.35	2.14	2
100	∞	1.46	–	–	–
500	10	1.65	1.7	1.4	1.7
500	∞	1.16	–	1.7	–
1000	50	1.41	1.16	1.51	1.32
1000	∞	1.1	–	1.61	–

Table 1 Drag and inertial coefficients for unidirectional and oscillatory flows

Flow Structure

The vorticity contours reflect the vortex formation and interaction around cylinders during each oscillation period. The vorticity contours of the single cylinder show half-period symmetry at $(KC, Re) = (10,500)$ (Figure 2a, b). In this type of vortex shedding regime, the flow structures at two times separated by half a period are symmetric across the y-axis. On the other hand, the flow structures of the cylinder in an array at two instants a half-period apart seem to be anti-symmetric with respect to the centre of the cylinder (Figure 2c, d). This regime has been referred to as "half period anti-symmetry" [1]. It can thus be seen that the presence of neighbour cylinders alters the flow structure at $(KC, Re) = (10,500)$.
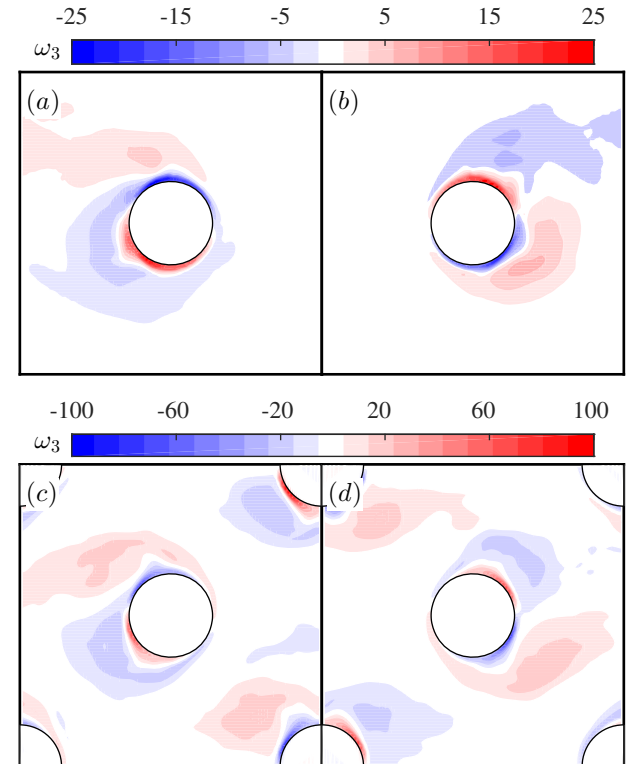
Figure 2 Instantaneous vorticity contours for $(KC, Re) = (10,500)$: (a) a single cylinder at $t/T = 0$; (b) a single cylinder at $t/T = 1/2$; (c) a cylinder in an array at $t/T = 0$ and (d) a cylinder in an array at $t/T = 1/2$

Investigating the non-dimensional pressure $p/\rho U_m^2$ distributions around the cylinders in oscillatory flow provides a better understanding of the mechanisms that produce transverse and streamwise forces. For $(KC, Re) = (5,100)$ at $t/T = 1/4$, the pressure distributions over both the single cylinder and the cylinder inside the array are similar, showing greater pressure forces in the transverse direction than in the streamwise direction (Figure 3a, c). On the other hand, at $t/T = 1/2$, the pressure distributions indicate strong streamwise pressure forces, which can be attributed to the strong flow acceleration at this phase angle (Figure 3b, d).
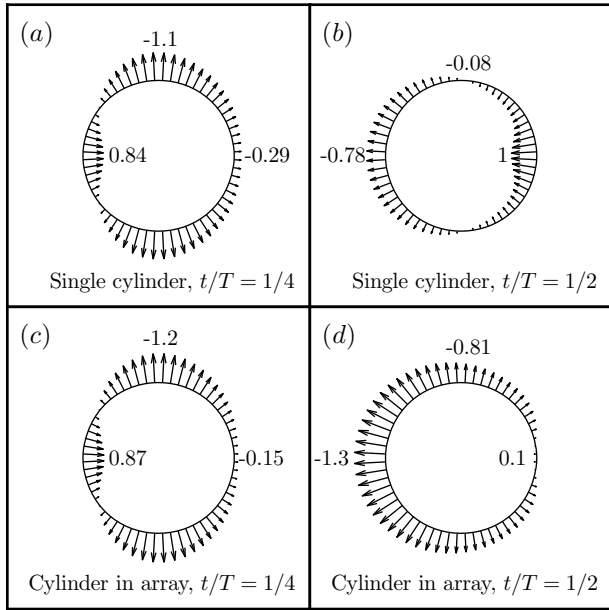
Figure 3 Non-dimensional pressure $p/\rho U_m^2$ distributions around a single cylinder (a and b) and a cylinder inside the array (c and d) at two time instants for $(KC, Re) = (5,100)$. Inward arrows indicate positive pressure.

The time-averaged velocity vectors and streamwise velocity contours demonstrate that, for oscillatory flow with $(KC, Re) = (10,500)$, four recirculating cells can be identified in the vicinity of cylinders (Figure 4a, b). It is evident that for given KC and Re, the flow velocity within the array of cylinders is much larger than that around the single cylinder. For unidirectional flow with $Re = 500$, there are two vortices formed in the wakes of the cylinders (Figure 4c, d). However, it can be seen that the vortices of the cylinder inside an array of cylinders are suppressed by the presence of neighboring cylinders. Similarly to oscillatory flow, the flow velocity within the array of cylinders is larger than the flow velocity around the single cylinder.

Ensemble-averaged values of streamwise force coefficients C_F $(= F_1/(\frac{1}{2}\rho U_m^2 d))$ along with dimensionless velocity curves $u_1 T/d$ are shown in Figure 5. As KC increases, the variation of C_F becomes more irregular and its amplitude decreases. The irregular behaviour of C_F at higher KC is due to the influence of shed vortices on the pressure distribution over the cylinder surface. Moreover, it can be seen that the amplitude of C_F oscillations for a single cylinder and a cylinder in an array are very similar except for $(KC, Re) = (50,1000)$ where C_F amplitude for cylinder in array is slightly larger. This is reflected in Table 1, which shows that both C_d and C_m values of a cylinder in an array are greater than those of a single cylinder for $(KC, Re) = (50,1000)$.
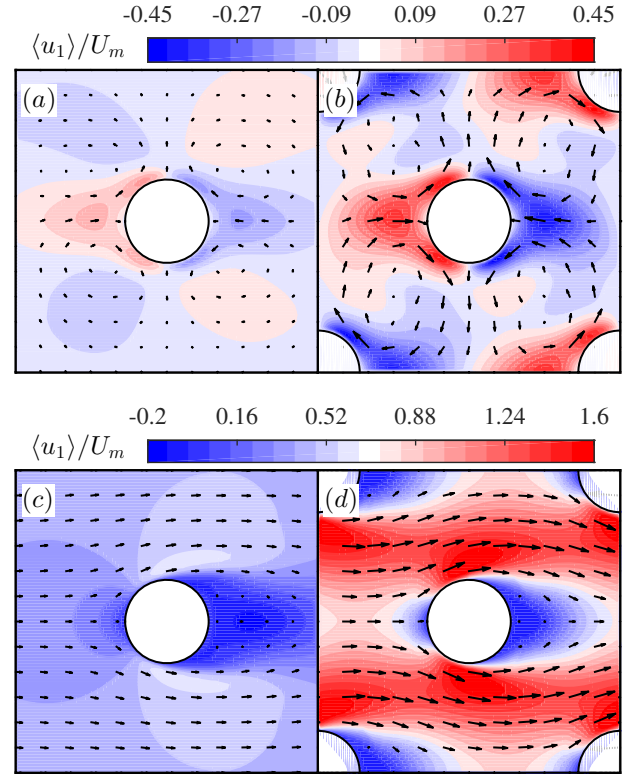
Figure 4 Time-averaged streamwise velocity contours and time-averaged velocity vectors (a) oscillatory flow over single cylinder, $(KC, Re) = (10,500)$; (b) oscillatory flow over array of cylinders, $(KC, Re) = (10,500)$; (c) unidirectional flow over a single cylinder, $Re = 500$; (d) unidirectional flow over array of cylinders, $Re = 500$.
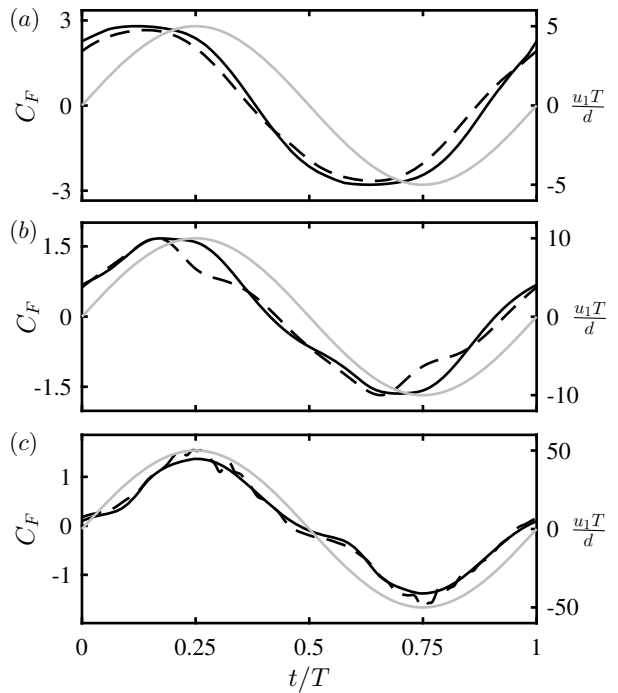
Figure 5 Phase-averaged values of streamwise force coefficients C_F and dimensionless velocity $u_1 T/d$ curves for (a) $(KC, Re) = (5,100)$ (b) $(KC, Re) = (10,500)$ (c) $(KC, Re) = (50,1000)$. The solid black lines, dashed black lines and solid grey lines show the single cylinder force coefficient, the force coefficient for a cylinder in an array and the dimensionless velocity, respectively.

Conclusions

The structure of oscillatory flow around, and streamwise forces exerted on, single cylinders and cylinders in an array were investigated. It was shown that in general, the drag coefficient C_d and inertia coefficient C_m of a cylinder in an array are significantly different to those of a single cylinder; this difference varies with KC and Re. Moreover, vorticity and streamwise velocity contours reveal that the structure of oscillatory flow around a single cylinder is significantly affected by the presence of neighbouring cylinders. The results of this study are beneficial for developing improved models for vegetation-induced wave attenuation.

References

[1] An, H., Cheng, L. and Zhao, M. Steady streaming around a circular cylinder in an oscillatory flow. *Ocean Engineering*, **36**, 2009, 1089-1097.

[2] Anderson, M. E. and Smith, J. M. Wave attenuation by flexible, idealized salt marsh vegetation. *Coastal Engineering*, **83**, 2014, 82-92.

[3] Camfield, F. E. Wind- wave growth with high friction. *Journal of Waterway, Port, Coastal & Ocean Engineering - ASCE*, **109**, 1983, 115-117.

[4] Dalrymple, R. A., Kirby, J. T. and Hwang, P. A. Wave diffraction due to areas of energy dissipation. *Journal of Waterway, Port, Coastal & Ocean Engineering - ASCE*, **110**, 1984, 67-79.

[5] Dütsch, H., Durst, F., Becker, S. and Lienhart, H. Low-Reynolds-number flow around an oscillating circular cylinder at low Keulegan-Carpenter numbers. *Journal of Fluid Mechanics*, **360**, 1998, 249-271.

[6] Houser, C., Trimble, S. and Morales, B. Influence of blade flexibility on the drag coefficient of aquatic vegetation. *Estuaries and Coasts*, **38**, 2015, 569-577.

[7] Hu, Z., Suzuki, T., Zitman, T., Uittewaal, W. and Stive, M. Laboratory study on wave dissipation by vegetation in combined current–wave flow. *Coastal Engineering*, **88**, 2014, 131-142.

[8] Infantes, E., Orfila, A., Simarro, G., Terrados, J., Luhar, M. and Nepf, H. Effect of a seagrass (Posidonia oceanica) meadow on wave propagation. *Marine Ecology Progress Series*, **456**, 2012, 63-72.

[9] Jadhav, R. S., Chen, Q. and Smith, J. M. Spectral distribution of wave energy dissipation by salt marsh vegetation. *Coastal Engineering*, **77**, 2013, 99-107.

[10] Kobayashi, N., Raichle, A. W. and Asano, T. Wave attenuation by vegetation. *Journal of Waterway, Port, Coastal, & Ocean Engineering - ASCE*, **119**, 1993, 30-48.

[11] Lima, S. F., Neves, C. F. and Rosauro, N. M. L. *Damping of gravity waves by fields of flexible vegetation*. City, 2007.

[12] Lowe, R. J., Falter, J. L., Koseff, J. R., Monismith, S. G. and Atkinson, M. J. Spectral wave flow attenuation within submerged canopies: Implications for wave energy dissipation. *Journal of Geophysical Research C: Oceans*, **112**, 2007.

[13] Lowe, R. J., Koseff, J. R. and Monismith, S. G. Oscillatory flow through submerged canopies: 1. Velocity structure. *Journal of Geophysical Research C: Oceans*, **110**, 2005, 1-17.

[14] Mendez, F. J. and Losada, I. J. An empirical model to estimate the propagation of random breaking and nonbreaking waves over vegetation fields. *Coastal Engineering*, **51**, 2004, 103-118.

[15] Morison, J. R., O'Brien, M. P., Johnson, J. W. and Schaaf, S. The force exerted by surface waves on piles. *Petroleum Transactions*, **189**, 1950, 149-154.

[16] Nehari, D., Armenio, V. and Ballio, F. Three-dimensional analysis of the unidirectional oscillatory flow around a circular cylinder at low Keulegan-Carpenter and β numbers. *Journal of Fluid Mechanics*, **520**, 2004, 157-186.

[17] Nepf, H. M. *Flow and transport in regions with aquatic vegetation*. City, 2011.

[18] Price, W. A., Tomlinson, K. W. and Hunt, J. N. The effect of artificial seaweed in promoting the build-up of beaches. *Coastal Engineering Proceedings*, **1**, 1968, 570-578.

[19] Stoesser, T., Kim, S. and Diplas, P. Turbulent flow through idealized emergent vegetation. *Journal of Hydraulic Engineering*, **136**, 2010, 1003-1017.

[20] Tanino, Y. and Nepf, H. M. Laboratory investigation of mean drag in a random array of rigid, emergent cylinders. *Journal of Hydraulic Engineering*, **134**, 2008, 34-41.

[21] Uzunoğlu, B., Tan, M. and Price, W. G. Low-Reynolds-number flow around an oscillating circular cylinder using a cell viscousboundary element method. *International Journal for Numerical Methods in Engineering*, **50**, 2001, 2317-2338.

[22] Weller, H. G., Tabor, G., Jasak, H. and Fureby, C. A tensorial approach to computational continuum mechanics using object-oriented techniques. *Computers in physics*, **12**, 1998, 620-631.

[23] Wolfram, J. and Naghipour, M. On the estimation of Morison force coefficients and their predictive accuracy for very rough circular cylinders. *Applied Ocean Research*, **21**, 1999, 311-328.

[24] Zeller, R. B., Weitzman, J. S., Abbett, M. E., Zarama, F. J., Fringer, O. B. and Koseff, J. R. Improved parameterization of seagrass blade dynamics and wave attenuation based on numerical and laboratory experiments. *Limnology and Oceanography*, **59**, 2014, 251-266.